SARS-CoV-2 infection of BNT162b2(mRNA)-vaccinated individuals is not restricted to variants of concern or high-risk exposure environments

Brittany Rife Magalis 1,2, Carla Mavian 1,2, Massimiliano Tagliamonte 1,2, Shannan N. Rich 1,3,4, Melanie Cash 1,2, Alberto Riva 5, Julia C. Loeb 1,6, Michael Norris 1,6, David Moraga 5, Yanping Zhang 5, Jerne Shapiro 3,4, Petr Starostik 2, Simone Marini 1,3, Paul Myers 4, David Ostrov 2, John A. Lednicky 1,6, J. Glenn Morris Jr. 1, Michael Lauzardo 1,4,7, Marco Salemi 1,2,[$],

1Emerging Pathogens Institute, University of Florida, Gainesville, FL, USA, 32610

2Department of Pathology, University of Florida, Gainesville, FL, USA, 32610

3Department of Epidemiology, College of Public Health and Health Professions and College of Medicine, University of Florida, Gainesville, FL, USA, 32610

4Florida Department of Health, Alachua County, Gainesville, FL, USA, 32641

5Bioinformatics Core, Interdisciplinary Center for Biotechnology Research, Gainesville, FL, USA, 32610

6Department of Environmental and Global Health, University of Florida, Gainesville, Florida 32610

7Division of Infectious Diseases and Global Medicine, College of Medicine, University of Florida, Gainesville, FL, USA, 32610

[$]Corresponding author

Abstract (150 words)

The emergence of SARS-CoV-2 variants of concern (VOC) has raised questions regarding the extent of protection of currently implemented vaccines. Ten “vaccination breakthrough” infections were identified in Alachua County, Florida, among individuals fully vaccinated with the

BNT162b2 mRNA vaccine as a result of social or household transmission. Eight individuals presented mild symptoms in the absence of infection with other common respiratory viruses, confirmed using viral genetic sequencing. SARS-CoV-2 genomes were successfully generated for five of the vaccine breakthroughs and 399 individuals in the surrounding area and were included for reference-based phylogenetic investigation. These five individuals were characterized by infection with both VOCs and low-frequency variants present within the surrounding population. Mutations, in the Spike glycoprotein, were consistent with their respective circulating lineages. However, we detected an additional mutation in Spike's N-terminal domain of a B.1.1.7 strain, present at low-frequency (~1%) in the unvaccinated population, potentially affecting protein's stability and functionality. The findings highlight the critical need for continued testing and monitoring of infection among individuals regardless of vaccination status.

Several rapidly spreading variants of severe acute respiratory syndrome coronavirus 2 (SARS-CoV-2) have risen to the status of "variants of concern" (VOC), according to the Centers for Disease Control (CDC, https://www.cdc.gov/coronavirus/2019-ncov/cases-updates/variant-surveillance/variant-info.html), accumulating as many as 17 unique genomic mutations with respect to the original viral strain originating from the Wuhan province of China (1). These VOCs include the lineages most notably defined by their area of origin, such as the United Kingdom (UK). The UK VOC, also referred to as the B.1.1.7 lineage using the Pango nomenclature (2), emerged in September of 2020 in Kent, UK, but quickly made its way to the United States (US, (3)). More recently, the B.1.427/B.1.429 lineages, two forms collectively dubbed the "California variant", were added to the CDC's list of VOCs, as they have spread widely since their initial detection in July of 2020 in Los Angeles County, California (4). The emergence of these and other VOCs, and their level of evolutionary divergence from the original strain, has raised questions regarding the extent of protection of currently implemented vaccines against infection

53 (5-8). Here, we report epidemiological and genomic data (where available) for vaccination
54 breakthrough cases from Alachua County, Florida, in the context of the diverse SARS-CoV-2
55 epidemic in Florida and the remaining US.

56

57 **Results**

58 From January to March 2021, Alachua County, Florida, experienced a reduced number of
59 infections (~11% drop in % positive cases), with a general increase in number of vaccinations,
60 particularly since the last week of February (**Figure S1**). Regardless of the reduced coronavirus
61 disease (COVID-19) burden in the county, continued testing of vaccinated individuals has
62 provided insight into susceptibility of vaccines to circulating viral variants within the region.
63 Between February and March 2021, ten individuals enrolled in the Screen, Test, & Protect
64 (STP) program (**online Methods**) tested positive using the standard polymerase chain reaction
65 (PCR)-based assay for SARS-CoV-2 infection after completing the BNT162b2 mRNA two-dose
66 vaccine series (9). Individuals were considered fully vaccinated two weeks after their second
67 vaccination in a 2-dose series. By March 17, 2021, more than 59,000 individuals were
68 vaccinated with at least one dose of one of Pfizer (49%), Moderna (49%), or Johnson &
69 Johnson (2%) vaccines in Alachua County, Florida (10). The number of infections among
70 vaccinated individuals suggests a relatively low breakthrough rate consistent with the high
71 efficacy of Pfizer's BNT162b2 vaccine demonstrated in clinical trials (9), though it is important to
72 acknowledge the small sample size of this study and potential sampling biases incorporated in
73 the STP program that limit drawing any conclusions regarding validation of efficacy (**online**
74 **Methods**). The ten "vaccine-breakthrough" individuals were all identified within 27-47
75 (mean=37.6) days following the second dose, eight of which presented with symptoms
76 characteristic of COVID-19 **(Tables 1** and **S1**). The majority of these individuals identified as
77 female (90%), White (80%), under the age of 35 (mean=34), and reported their occupation as

healthcare-related (80%), including students working in patient care. Contact tracing revealed that seven of these individuals had exposures to individuals previously identified as COVID-19 cases in the two weeks prior to their disease onset, with four reporting the nature of the relationship as household and three as community/social. None of the individuals reported exposure in the workplace. So, despite healthcare workers increased risk of exposure, infection in these individuals was likely the result of inadvertent exposure during social contact.

Saliva samples were collected from the ten vaccine-breakthrough individuals within 3-7 days of testing positive for infection (**Tables 1** and **S1**). Saliva collection was used in this study for the isolation of viral RNA, as this bodily fluid has demonstrated prolonged presence of viral RNA (up to 25 days post-symptom onset, (11)), irrespective of disease severity (12). The research protocol (**online Methods**) was approved by the University of Florida institutional review board. SARS-CoV-2 full-genome (>70%) sequences were successfully generated for five of the vaccinated individuals. A panel of additional respiratory viruses was also targeted during sequencing (**Table S2**), confirming the absence in all patients of additional infection with common viruses, such as influenza. Thus, clinical symptoms, when present, were likely the result of productive coronavirus infection. The reason for insufficient SARS-CoV-2 genome quality for five of the vaccine breakthrough cases is not fully clear. Results from COVID-19 testing for the majority of these individuals were limited to qualitative data (positive or negative), though the number of PCR cycles (Cq) required for reliable viral RNA amplification for two of the individuals were provided and already >25 at the time of diagnosis (**Table S3**), which has been considered relatively high for genomic sequencing (13). Given the time between diagnosis and saliva sampling (**Table S1**), saliva viral load may have been too low for the genomic amplification required for amplicon-based sequencing for some individuals. While mutations in primer-binding regions can reduce genome coverage for amplicon-based sequencing (13),

103 coverage mapping did not indicate this phenomenon – alternating regions of high- and low-
104 coverage were not observed (**Figure S2**). Two of these individuals were, however,
105 asymptomatic whereas asymptomatic individuals were not found among the successful full-
106 genome sequences (**Table S2**), supporting the link between severity of symptoms and rapidity
107 of viral clearance (14).
108
109 In order to understand the context of the vaccine breakthrough infections, we assembled a full-
110 genome sequence dataset (n=3902) including sequences generated from hospital samples in
111 Alachua County between January-March 2021 (n=399), all Floridian sequences (n=3,016)
112 deposited into the GISAID database (https://gisaid.org), and epidemiologically relevant
113 sequences from the global population (also from GISAID). Epidemiological relevance was
114 defined on an individual sequence basis, restricting the global GISAID search to the two
115 sequences most similar genetically to each Floridian sequence and sampled within a high-
116 confidence transmission time window (30 days) based on sample collection date. Additional
117 details on this method (termed "FLACO-BLAST") can be found in the **online Methods** and (15),
118 and the script is available from https://github.com/salemilab/flaco. GISAID IDs and
119 corresponding submission information are provided in **Table S4**. Owing to low genetic
120 variability, as well as potentially shared epidemiological linkages, sequences retrieved from
121 GISAID were often shared by more than one query (Florida) sequence, resulting in a total of
122 482 non-Floridian sequences, all of which were located within the US. The resulting dataset
123 spanned October 10, 2020 to March 17, 2021.
124
125 Lineages for all sequences were determined using the PangoLEARN model (Pangolin v 2.3.6),
126 which was trained using ~60,000 GISAID SARS-CoV-2 sequences to classify incoming
127 sequences based on molecular and epidemiological criteria (2). The full dataset in this study
128 was characterized by a total of 106 lineages, for which only nine (B.1.X) lineages

129 represented >99% of samples (**Figure 1A**). The distribution of lineages for Floridian sequences
130 outside of Alachua County largely resembled that of the non-Floridian reference sequences, as
131 expected given the filtering approach for genetic similarity described above; the exception to this
132 similarity was the presence of the B.1.375 lineage within the Florida dataset, which was not
133 present among reference sequences (**Figure 1A**). As this lineage was not observed among the
134 Alachua County sequences, further investigation into the potential misclassification of these
135 sequences as the B.1.375 lineage, more notably associated with the northern states (16), was
136 considered outside the scope of this study. Whereas both the Alachua County and remaining
137 Floridian samples were dominated by the B.1.234 lineage in November 2020, both regions
138 quickly expanded to include at least seven other lineages by mid-January 2021 (**Figure 1A**).
139 This expansion included a growing presence of the B.1.1.7 (or UK VOC) and B.1.427 (California
140 VOC) lineages (**Figure 1A**). Given the growth in the UK and California variants within the
141 Florida population, it is not surprising that three of the vaccinated individuals reported in this
142 study were determined to belong to these VOCs – 1 B.1.1.7 and 2 B.1.247/B.1.249. The
143 remaining two vaccinated individuals, however, presented with the high-frequency (~16%) B.1
144 lineage and low-frequency (<1%) B.1.377 lineage, neither of which is considered a VOC.
145
146 Following lineage classification, a maximum likelihood phylogenetic tree was reconstructed from
147 the sequences in order to verify lineage classification and to determine relationships among
148 vaccinated individuals in the context of geographical and temporal information (**Figure 1B**).
149 Bootstrap replicates for the sequence data were used to provide support for branching patterns
150 within the tree (17-19), and the smallest (number of sequences), well-supported (>90% of
151 replicates) clade involving each vaccination-breakthrough case was examined individually.
152 Whereas four of the five successfully sequenced, vaccinated individuals belonged to relatively
153 small, definable clades (**Figure 1C-D**), reliable placement of the fifth B.1-lineage individual
154 within the tree could not be obtained, despite >90% coverage of the genome (**Figure S2**). This

155 sequence did, however, share common ancestry with similarly B.1 sequences, supporting
156 proper lineage assignment (**Figure S3**). The two individuals harboring the B.1.429 California
157 VOC belonged to a clade of 20 individuals comprised of additional B.1.429/B.1.427 variants,
158 confirming lineage classification using Pangolin (**Figure 1C**). The remaining 18 sequences
159 within this clade consisted primarily of Floridian sequences (nine from Alachua County), with the
160 exception of one individual from Minnesota, suggesting largely local transmission of this variant,
161 though directionality of transmission cannot be inferred. The two vaccine-breakthrough cases
162 with the B.1.429 VOC in this study (STP-413 and STP-412) reported separate exposures; the
163 two individuals were also not more closely related to each other phylogenetically than the
164 remainder of the sequences (with significant support), so we can neither confirm nor exclude the
165 possibility of a relationship via direct transmission between these two individuals specifically.
166
167 Circulation of the other VOC in the US, B.1.1.7, has been defined as the result of at least two
168 separate introductions (3). One introduction was estimated to occur early November, 2020, into
169 California, and was characterized by a virus resembling more closely the traditional UK variant.
170 The second introduction, estimated to occur in late November, carried a silent mutation from
171 cytosine to thymine within the ORF1ab gene encoding the RNA-dependent RNA polymerase
172 (position 15720 relative to genome start). The expanding virus populations originating from
173 these two events were referred to as “Clade 1” and “Clade 2.” Approximately 13% of B.1.1.7
174 individuals within the total Florida sample, and 86% of B.1.1.7 in Alachua County, harbored the
175 “Clade 2” C15720T mutation, including the vaccine-breakthrough case. This individual (STP-11)
176 belonged to a well-supported clade in this study comprised of five total individuals (**Figure 1D**),
177 all sharing the B.1.1.7 lineage designation (again confirming pangolin classification) and “Clade
178 2” mutation. Despite the prevalence of the “Clade 2” mutation among B.1.1.7 individuals in
179 Alachua County, only one other sample within the vaccine-breakthrough clade originated from

180 the county. The remaining four samples were collected in Pennsylvania, New York, and New
181 Jersey, consistent with the earlier evidence of a more widespread presence of this B.1.1.7
182 variant within the US (3). The individual was reportedly exposed to a recent COVID-19 case
183 outside of the household. Contact tracing of this individuals' exposed contacts did not identify
184 any secondary cases associated with this vaccine failure, and so the question of ongoing
185 transmission following infection in this individual remains unanswered.
186
187 The final clade containing the low-frequency B.1.377 vaccinated individual (STP-410) shared
188 significant common ancestry with a single Floridian B.1.377 sequence, confirming lineage
189 classification and suggesting transmission within Florida, but not confined to the county (**Figure**
190 **1E**).
191
192 Even though infection in fully vaccinated individuals does not appear to be related to the viral
193 variant, mutational analysis was necessary to determine if 1) recently acquired mutations (i.e.,
194 not conserved among the corresponding lineage) could potentially be responsible for limited
195 protection of the vaccine against infection or 2) evidence exists for the emergence of vaccine-
196 resistant variants. The viral protein commonly referred to as the Spike protein is structurally
197 important for coronaviruses, rendering it susceptible to recognition by the host immune
198 response, specifically the receptor-binding domain (RBD). For this reason, vaccination efforts
199 have largely focused on this region of the genome (9, 20, 21), though there is evidence that the
200 host immune system can also target the N-terminal domain (NTD, (22, 23)). The natural
201 accumulation of mutations in these regions owing to the error-prone viral replication machinery
202 can lead to the ability of the virus to evade the host immune response, including that of
203 vaccinated individuals, and may be responsible for enhanced transmissibility of the variant (24).
204 The B.1.429 and B.1.377 variants found within three of the breakthrough-vaccinated individuals
205 did not appear to have acquired any additional Spike mutations outside of those associated with

206 the parental lineage, suggesting newly acquired mutations were not responsible for
207 breakthrough infections and that this individual did not harbor a vaccine-resistant variant.
208 However, two mutations relative to the parental B.1.1.7 lineage (1) were observed within the
209 Spike protein for the B.1.1.7 vaccinated individual – L18F and K1191N within the NTD and C-
210 terminal domain (CTD) of the Spike protein, respectively (**Figure 2A,** corresponding to positions
211 within the reference sequence MN908947). The HR2 K1191N mutation was present in ~75% of
212 samples for Alachua County, ~75% of the remainder of Florida samples, and ~75% of US
213 reference sequences, suggesting a less recent acquisition of this mutation in the population and
214 no relation to vaccine-mediated adaptation or an enhanced ability to infect vaccinated
215 individuals. Alternatively, the NTD L18F mutation was far less prevalent, only observed in 16
216 individuals from Florida (dating back to January 15, 2021), but not from the Alachua County
217 area (**Figure 2B**). It was known that the B.1.1.7 vaccination-breakthrough individual (STP-11)
218 was exposed to an infected individual from Orange County, Florida, which suggests a regional
219 Florida outbreak with this particular mutation that spilled over into Alachua County. No evidence
220 of secondary cases associated with this individual again cannot confirm ongoing transmission of
221 this variant among vaccinated individuals, though this mutation may warrant further investigation
222 for its antigenic properties and relationship to vaccination efficacy.
223
224 Several molecular vaccine and/or antigenic studies in the context of the B.1.1.7 variant have
225 focused on the RBD, demonstrating no significant effect on neutralization of the virus (25) and
226 no loss of affinity for host antibodies (Abs) to the RBD when compared to the original strain.
227 Meanwhile, mutations in the NTD (other than L18F) have been proposed to alter Ab affinity,
228 potentially paving the way for infection in vaccinated individuals (20). The structural
229 consequence of the recently acquired NTD L18F mutation indicates that this Floridian B.1.1.7
230 variant may be a variant of concern. In addition to B.1.1.7 deletions that eliminate antigenic
231 epitopes for neutralizing antibodies (26) and T cells (Δ69-70, Δ144), this variant exhibits an

232 amino acid change with the potential to stabilize the NTD of the Spike protein. Amino acid
233 position 18 is located within the N1 loop (residues 14 to 26), wherein the original L (Lysine) is
234 oriented towards F (Phenylalanine) at position 79 of the N2 loop (residues 67 to 79, **Figure 3A**).
235 The change from L to F in the Florida B.1.1.7 variant is predicted to form stabilizing contacts
236 between F18 in the N1 loop and S252 in the N5 loop (residues 246 to 260) (**Figure 3B**). These
237 data suggest that the Floridian B.1.1.7 variant found in the B.1.1.7 vaccinated individual may
238 exhibit a fitness advantage that results from increased stability and functionality of the NTD.
239
240 In order to verify viability of this new mutation, infectivity of the virus isolated from individual
241 STP-11 was measured *in vitro* (**online Methods**). Positive infection, and thus viability, was
242 defined by the presence of virus-specific cytopathic effects (CPE) on Vero E6 cells (African
243 green monkey kidney cells). CPE were first noted 12 days post-inoculation (dpi), primarily
244 consisting of rounding of cells, some in the process of detaching from the growing surface
245 (**Figure 4**). Quantification of virus at 12 dpi for the STP-11 sample-infected cells and control (no
246 viral inoculation) confirmed viral replication (C_q 8.14 and C_q > 39, respectively).
247
248 **Discussion**
249 A recent study in Israel reported that vaccinated individuals were disproportionally infected with
250 VOCs relative to the unvaccinated population (27). Whereas we cannot exclude the impact of
251 prevalence of VOCs within the Florida population on their rate of breakthrough, the findings of
252 our study, collectively with (27), indicate limited protection of the BNT162b2 mRNA vaccine (and
253 potentially others) against emerging variants of SARS-CoV-2. It is important to note that none of
254 the breakthrough individuals in this study was hospitalized, corroborating the vaccine's 100%
255 efficacy against severe disease (9). While these individuals presented with only mild symptoms
256 (or no symptoms at all), the number of vaccine breakthrough cases might be expected to be
257 under-reported. Hence, if we assume at least a minority of test-positive vaccinated individuals

258 harbor infectious virus, the potential for hidden reservoirs within the global populations is
259 increased. Hidden reservoirs in asymptomatic or mild symptomatic individuals, as has been
260 proposed (15), pose a particular threat to early recognition of mutations of potential concern,
261 such as the L18F mutation described herein, particularly once vaccination is more widespread.
262 Moreover, given the effectiveness of the vaccine in limiting symptom presentation, vaccinated
263 individuals may engage more frequently in social activities, increasing the risk of exposure.
264 Continued testing and case management, assessing contacts and exposure, for vaccinated
265 individuals is thus encouraged and will be forthcoming in determining whether the vaccine is
266 protective against ongoing evolution and spread of SARS-CoV-2. This strategy is particularly
267 important in the face of relaxed guidelines regarding masked protection and social distancing for
268 vaccinated individuals, declared by the CDC as of May, 2021.
269

270 **Acknowledgments**

271 This work was supported by the Stephany W. Holloway University of Florida Chair and by funds
272 of the University of Florida Office of Research and Health Science Center with resources from
273 the Interdisciplinary Center for Biotechnology Research Gene Expression Core
274 (RRID:SCR_019145), NextGen Sequencing Core (RRID:SCR_019152) and Bioinformatics Core
275 (RRID:SCR_019120).
276

277 **Table 1. Reported cases of vaccination breakthroughs in Alachua County, Florida.**

Characteristic	
Age (years)	34.0 (15.0)
Sex	
Female	9 (90.0%)
Race	
White	8 (80.0%)
Ethnicity	
Hispanic	2 (20.0%)
Symptoms (Y)	8 (80.0%)
Cough	1 (12.5%)

Anosmia	1 (12.5%)
Sore throat	3 (37.5%)
Headache	4 (50.0%)
Runny nose	5 (62.5%)
Fatigue	2 (25.0%)
Comorbidities	
Asthma	1 (10.0%)
BMI	24.6 (5.0)
Known exposure (Y)	7 (70.0%)
Household	4 (57.1%)
Community	3 (42.9%)
Occupation	
Healthcare worker	7 (70.0%)
Student engaged in patient care	2 (20%)
Unemployed	1 (10%)
Time between second vaccination dose and disease onset (days)	37.6 (21.3)
Time between disease onset (for symptomatic cases) and sample collection date (days)	5.0 (2.0)

*Results are presented as frequency (%) for categorical variables and mean (standard deviation) for continuous variables.

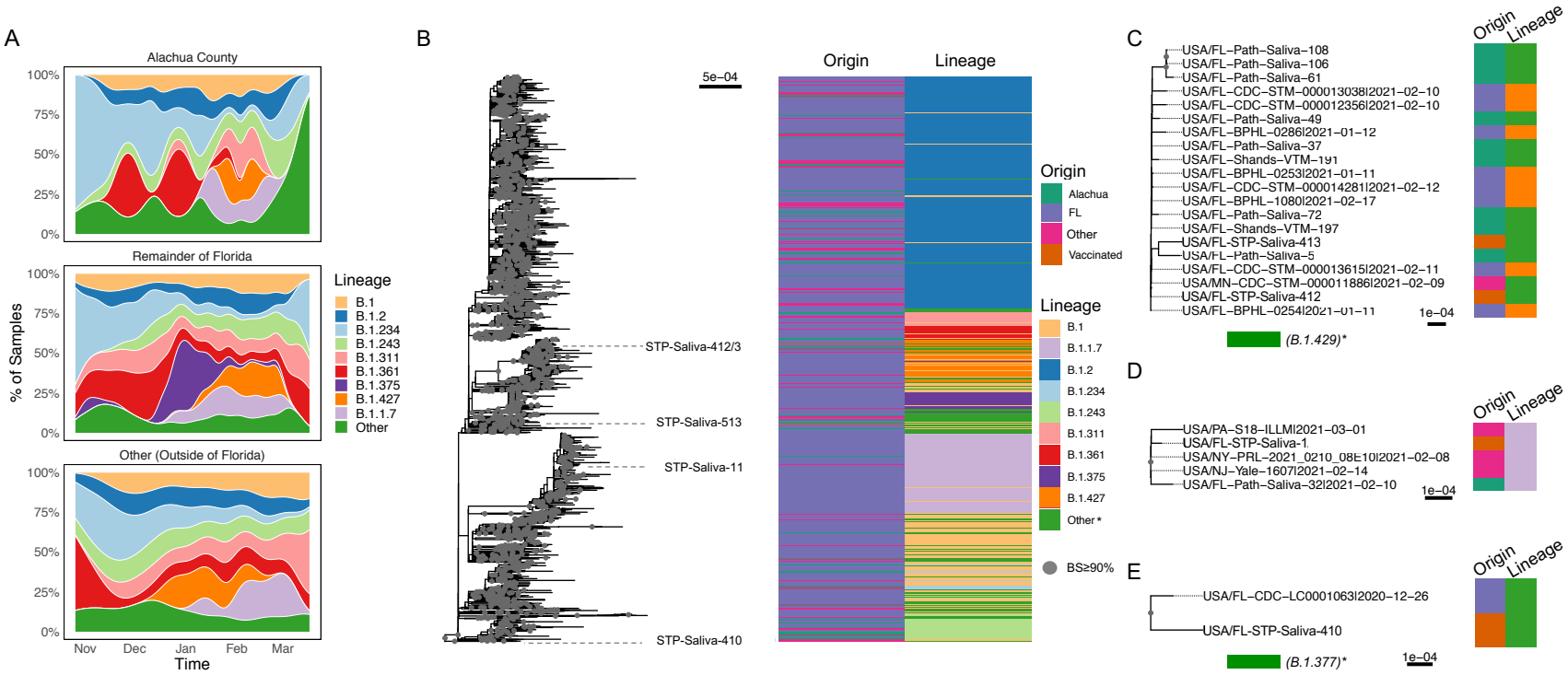

Figure 1. Distribution of identified lineages and geographical origin of sampling over time (A) and within the phylogenetic tree (B-D) of SARS-CoV-2 data collected from Florida and relevant non-Florida locations. (A) Lineage (as identified using Pangolin (2) distribution over time for Alachua County, the surrounding Florida areas, and locations outside of Florida linked to Florida sequences via genetic similarity. (B) Distribution of both assigned lineages and geographic origin (as in (A)) across the maximum likelihood phylogenetic tree. Branches are scaled in genetic substitutions/site, and nodes with ≥90% support using bootstrap sampling are indicated by grey dots. Vaccinated individuals within well-supported clades have been emphasized, and corresponding clades are represented as insets in panels C-D. *Other lineages, defined as present within <1% of the total sample population.

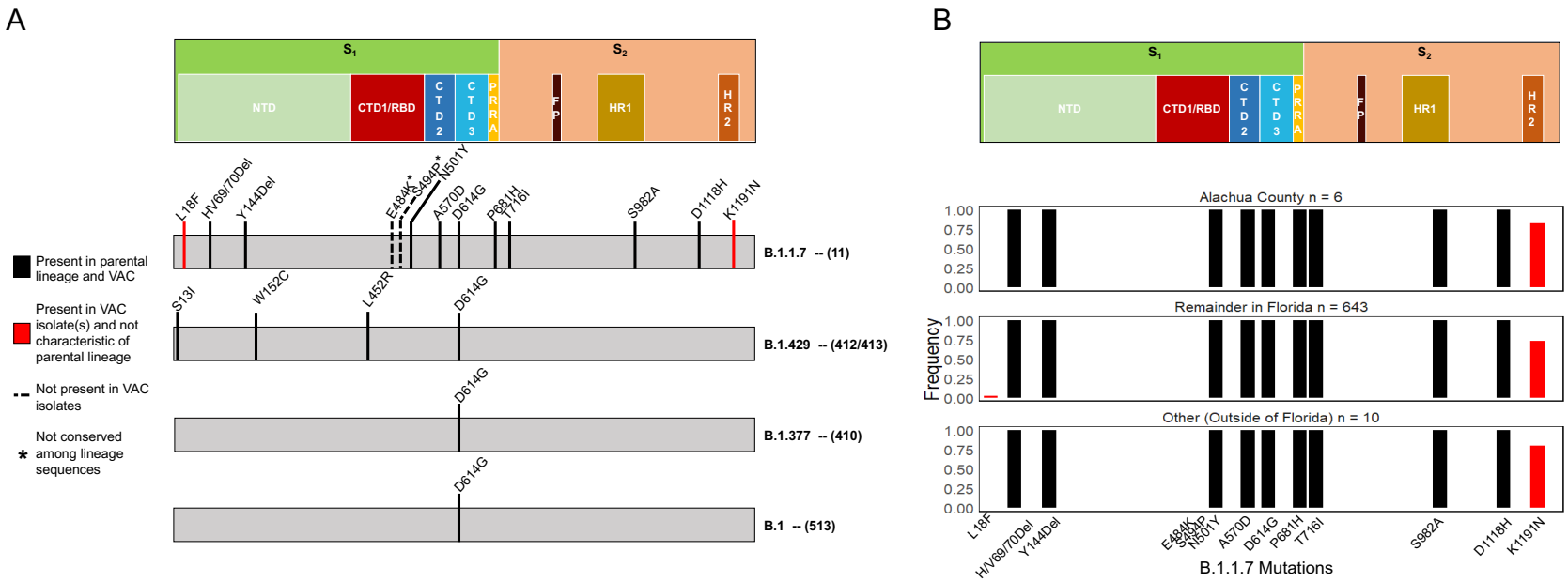

Figure 2. Mutational profiles for vaccine-breakthrough individuals (A) and comparison of B.1.1.7 individuals with remaining sequence data (B). Mutations in red are present in vaccinated individual (VAC), but not fixed in the parental lineage. Spike protein architecture is displayed at the top of both panels, wherein S = spike subunit (1-2); NTD = N-terminal domain; CTD (1-3) = C-terminal domain; RBD = receptor binding domain; PRRA = SARS-CoV-2 characteristic PRRA insertion at the S_1/S_2 cleavage site; FP = fusion peptide; HR (1-2) heptad repeat. Positions numbers are relative to the Spike protein in the MN908947 reference sequence.

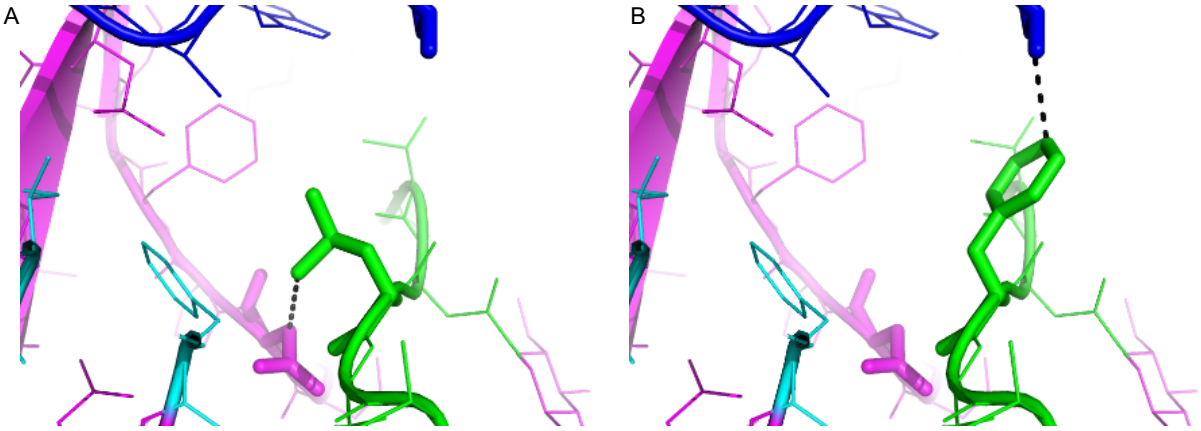

Figure 3. Potential stabilizing effect of Floridian B.1.1.7 variant mutation from Lysine (A) to Phenylalanine (B) at position 18 of the Spike protein N-terminal domain (NTD). Loops N1, N2, and N5 of the NTD are represented in green, pink, and blue, respectively. Modified interactions as a result of the mutation are represented as dotted lines, with original L18 oriented toward position F79 (cyan) of the N1 loop (A), and the variant F18 toward S252 of the N5 loop (B), potentially acting to stabilize. Dotted lines represent distances 3.8 (A) and 3.6 (B) Angstrom. Positions numbers are relative to the Spike protein in the MN908947 reference sequence.

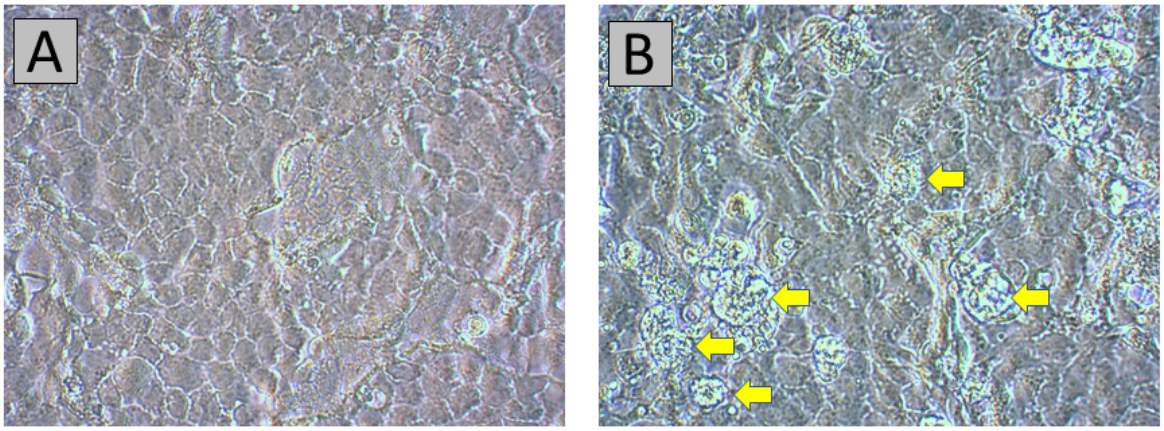

Figure 4. Cytopathic effects in Vero E6 cells inoculated with saliva sample FL-STP-Saliva-11. (A) Mock-infected Vero E6 cells, 12 dpi. (B) Early SARS-CoV-2-specific CPE, 12 dpi. Rounded cells, some in the process of detaching from the growth surface, are pointed out by yellow arrows. Original magnification at 400X.

318 **Methods**

319

320 **Participant involvement and sample processing.** Individuals deemed PCR-positive for
321 SARS-CoV-2 by a clinician affiliated with the University of Florida in Alachua County were
322 eligible for molecular epidemiology investigation as part of the statewide Screen, Test, and
323 Protect (STP) program if they met the following criteria:

324 1) The case must be infectious at the time of saliva sample donation

325 2) The case must meet the definition of a vaccine-breakthrough case or be involved in a
326 cluster of concern and the molecular epidemiology investigation is approved by STP leadership.

327 If both criteria were met and informed consent for the use of the sample for the purpose of
328 public health molecular surveillance was given, individuals were encouraged to arrive on site for
329 sample collection as soon as possible to increase the probability of detectable virus for
330 collection. Each participant was asked to give a saliva sample of at least 2 mL in total volume
331 and was instructed not to drink anything for 10 minutes prior to giving the sample. The saliva
332 was collected in a 15 mL conical tube, filling it to the 2 mL marking on the tube, not including
333 froth. Patient samples were de-identified following Institutional Review Board approval prior to
334 viral processing. Viral RNA was extracted from 180 uL of each saliva sample using the QIAamp
335 96 Viral RNA Kit with the QIAcube HT (Qiagen, Germantown, MD) using the following settings
336 with a filter plate: the lysed sample was premixed 8 times before subjecting to vacuum for 5
337 minutes at 25kP and vacuum for 3 min at 70kPa. Following 3 washes using the same vacuum
338 conditions above, the samples were eluted in 100 uL AVE buffer followed by a final vacuum for
339 6 minutes at 60kPa. Nine microliters of RNA was used for cDNA synthesis and library
340 preparation using the COVIDSeq Test kit (Illumina, San Diego, CA) and Mosquito HV Genomics
341 Liquid Handler (SPT Labtech Inc., Boston MA). The size and purity of the library was
342 determined using the 4200 TapeStation System (Agilent, Santa Clara, CA) and the Qubit

343 dsDNA HS Assay Kit (Life Technologies, Carlsbad, CA) according to the manufacturer's
344 instructions. Constructed libraries were pooled and sequenced using the NovaSeq 6000
345 Sequencing System SP Reagent Kit and the NovaSeq Xp 2-Lane Kit. Illumina's DRAGEN
346 pipeline was used to derive sample consensus sequences, which were filtered based on a
347 minimum of 70% coverage of the genome.

348

349 **Database sequence retrieval.** Each Floridian sequence was used in a local alignment (BLAST)
350 (28) search for the most (genetically) similar non-Floridian sequence in the GISAID database as
351 of March 23, 2021, and linked to two reference sequences including the best match (highest E-
352 value) with a date occurring within one month following, as well as one month prior to the
353 sampling date of the Floridian sequence (15). After removing duplicate sequences (sequences
354 with same GISAID ID), sequences were aligned in viralMSA (29) using the MN908947 reference
355 sequence, and mutations potentially associated with contamination, recurrent sequencing
356 errors, or hypermutability were masked using a vcf filter (https://virological.org/t/masking-
357 strategies-for-sars-cov-2-alignments/480).

358

359 **Cell culture for viral infectivity.** Vero E6 cells were used for SARS-CoV-2 isolation attempts.
360 The cells had been obtained from the American Type Culture Collection (catalog no. ATCC
361 CRL-1586) and have been used for our SARS-CoV-2 projects (30-33), including the isolation
362 of > 30 SARS-CoV-2 isolates from human and environmental samples. The cells were
363 propagated in cell culture medium comprised of aDMEM (advanced Dulbecco's modified
364 essential medium, Invitrogen, Carlsbad, CA) supplemented with 10% low antibody, heat-
365 inactivated, gamma-irradiated fetal bovine serum (FBS, Hyclone, GE Healthcare Life Sciences,
366 Pittsburgh, PA), L-alanine, L-glutamine dipeptide supplement (GlutaMAX,), and 50 µg/mL

367 penicillin, 50 µg/mL streptomycin, 100 µg/mL neomycin (PSN antibiotics, Invitrogen) with
368 incubation at 37°C in 5% CO_2.
369
370 **Isolation of virus in cultured cells.** Virus isolation attempts were performed in a BSL3
371 laboratory at the University of Florida Emerging Pathogens Institute (EPI) by analysts who wore
372 powered air-purifying respirators and engaged in BSL3 work practices. Vero E6 cells grown as
373 monolayers in a T-25 flask (growing surface 25 cm^2) were inoculated when they were at 80% of
374 confluency as follows: for each flask, the spent cell culture medium was removed and replaced
375 with 1 mL of supplemented aDMEM medium ("complete medium") with 10% FBS, and the cells
376 inoculated with 50 µL of unfiltered saliva. Prior to inoculation, samples were frozen (-80°C)
377 within 15 minutes following collection. Samples were only thawed once to produce an aliquot for
378 processing. The inoculated cell cultures were incubated at 37°C in 5% CO_2, and rocked every
379 15 minutes for 1 hour, after which 4 mL of complete medium with 10% FBS was added. The
380 following day, the cell culture media was completely removed and replenished with 5 mL of
381 maintenance medium (complete medium with 3% FBS). Mock-infected cell cultures were
382 maintained in parallel with the other cultures. The cell cultures were refed every 3 days by the
383 replacement of 2 mL of spent media with maintenance medium. The cells were observed daily
384 for one month before being judged negative for virus isolation, with a blind passage performed
385 15 days post-inoculation of the cells. When virus-induced cytopathic effects (CPE) were evident,
386 the presence of SARS-CoV-2 in the cell culture medium was examined by real-time reverse
387 transcription PCR (rRT-PCR). In the event that SARS-CoV-2 strains that were not cytolytic or
388 did not produce CPE had been isolated, the culture media were blindly tested at weekly
389 intervals.
390
391 **Detection of SARS-CoV-2 genomic RNA (vRNA) in cell culture medium.** vRNA was
392 extracted from virions in collection media in a Class II biosafety cabinet in a BSL3 laboratory at

393 the EPI by analysts wearing appropriate personal protective equipment (chemically impervious
394 Tyvek lab coats and gloves) and using powered-air purifying respirators. The vRNA was
395 extracted from 140 µL aliquots of the collection media using a QIAamp Viral RNA Mini Kit
396 (Qiagen, Valencia, CA, USA), and purified RNA eluted from the RNA-binding silicon column in a
397 volume of 80 µL. Twenty-five µL (final volume) rRT-PCR tests were performed in a BioRad
398 CFX96 Touch Real-Time PCR Detection System using 5 µL of purified vRNA and the N1 and
399 N2 primers and their corresponding probes of the CDC 2019-Novel Coronavirus (2019-nCoV)
400 rtRT-PCR test (34). The primers and probes were purchased from Integrated DNA
401 Technologies (IDT, Coralville, Iowa, USA). A plasmid that encodes the SARS-CoV-2 N-gene
402 sequence was purchased from IDT and used in positive control reactions for the CDC N1 and
403 N2.
404 The rRT-PCR tests were performed using the following parameters: 400 nM final
405 concentration of forward and reverse primers and 100 nM final concentration of probe using a
406 SuperScript III One-Step RT-PCR system with Platinum Taq DNA Polymerase (ThermoFisher
407 Scientific). Cycling conditions were 20 minutes at 50°C for reverse transcription, followed by 2
408 minutes at 95°C for Taq polymerase activation, then 45 cycles of denaturation for 15 seconds at
409 95°C, annealing for 30 seconds at 55°C, and extension at 68°C for 20 seconds.
410
411 **Table S1. Sample and sequencing information for vaccinated (VAC) individuals.**

VAC-ID	Time between second vaccination dose and disease onset[a] (days)	Time between onset[b] and sample collection (days)	Symptom status	Exposure	Lineage
STP-Saliva-11	31	4	Symptomatic	Community	B.1.1.7
STP-Saliva-410	36	6	Symptomatic	Household	B.1.377
STP-Saliva-409	32	4	Symptomatic	Household	Undetermined
STP-Saliva-412	37	6	Symptomatic	Community	B.1.429
STP-Saliva-413	35	7	Symptomatic	Household	B.1.429
STP-Saliva-411	47	3	Asymptomatic	Household	Undetermined
STP-Saliva-512	27	5	Symptomatic	Unknown	Undetermined
STP-Saliva-511	51	1	Asymptomatic	Unknown	Undetermined

STP-Saliva-514	39	7	Symptomatic	Community	Undetermined
STP-Saliva-513	41	7	Symptomatic	Unknown	B.1

[a]Onset implies the date of symptom onset for symptomatic individuals or the date of lab collection for the result of virus detection among asymptomatic individuals.

Table S2. Respiratory virus coverage during sequencing of saliva samples from vaccine-breakthrough individuals.

VAC-ID	Virus	Total Coverage[a]	Median Coverage[b]
STP-Saliva-11	Influenza B virus (B/Brisbane/60/2008)	17369	0
	Influenza A virus (A/Michigan/45/2015(H1N1))	2368	0
	Influenza B virus (B/Wisconsin/01/2010)	1352	0
	Influenza A virus (A/Texas/50/2012(H3N2))	874	0
	Influenza B virus (B/Washington/02/2019)	50	0
STP-Saliva-409	Influenza B virus (B/Brisbane/60/2008)	843	0
	Influenza A virus (A/Michigan/45/2015(H1N1))	139	0
	Influenza A virus (A/Texas/50/2012(H3N2))	27	0
	Influenza B virus (B/Wisconsin/01/2010)	24	0
	Influenza B virus (B/Lee/1940)	12	0
STP-Saliva-410	Influenza B virus (B/Brisbane/60/2008)	9748	0
	Influenza A virus (A/Michigan/45/2015(H1N1))	1310	0
	Influenza A virus (A/Texas/50/2012(H3N2))	656	0
	Influenza B virus (B/Wisconsin/01/2010)	480	0
	Human coronavirus HKU1	88	0
	Influenza B virus (B/Washington/02/2019)	57	0
	Human coronavirus NL63	35	0
	Human adenovirus B1	27	0
	Human adenovirus E4	14	0
	Influenza A virus (A/Puerto Rico/8/1934(H1N1))	12	0
STP-Saliva-411	Influenza B virus (B/Brisbane/60/2008)	801	0
	Influenza A virus (A/Michigan/45/2015(H1N1))	109	0
	Influenza A virus (A/Texas/50/2012(H3N2))	79	0
	Influenza B virus (B/Wisconsin/01/2010)	26	0
	Human adenovirus B1	23	0
	Influenza A virus (A/Puerto Rico/8/1934(H1N1))	12	0
STP-Saliva-412	Influenza B virus (B/Brisbane/60/2008)	14738	0
	Influenza A virus (A/Michigan/45/2015(H1N1))	2055	0
	Influenza A virus (A/Texas/50/2012(H3N2))	1447	0
	Influenza B virus (B/Wisconsin/01/2010)	1065	0
	Influenza B virus (B/Washington/02/2019)	54	0

	Human adenovirus C2	35	0
	Influenza B virus (B/Lee/1940)	13	0
STP-Saliva-413	Influenza A virus (A/Michigan/45/2015(H1N1))	6848	0
	Influenza B virus (B/Brisbane/60/2008)	5036	0
	Influenza A virus (A/Texas/50/2012(H3N2))	306	0
	Influenza B virus (B/Wisconsin/01/2010)	241	0
	Human adenovirus C2	36	0
	Human coronavirus NL63	25	0
	Human metapneumovirus (CAN97-83)	24	0
	Human adenovirus E4	22	0
	Human parainfluenza virus 3	13	0
	Influenza A virus (A/Puerto Rico/8/1934(H1N1))	12	0
STP-Saliva-511	Influenza B virus (B/Brisbane/60/2008)	1269	0
	Influenza A virus (A/Michigan/45/2015(H1N1))	168	0
	Influenza A virus (A/Texas/50/2012(H3N2))	62	0
STP-Saliva-512	Influenza B virus (B/Brisbane/60/2008)	133	0
	Influenza B virus (B/Wisconsin/01/2010)	87	0
	Influenza A virus (A/Michigan/45/2015(H1N1))	51	0
	Human adenovirus C2	12	0
	Human adenovirus B1	12	0
	Human bocavirus 4 NI strain HBoV4-NI-385	12	0
STP-Saliva-513	Influenza B virus (B/Brisbane/60/2008)	5498	0
	Influenza A virus (A/Michigan/45/2015(H1N1))	1550	0
	Influenza A virus (A/Texas/50/2012(H3N2))	551	0
	Influenza B virus (B/Wisconsin/01/2010)	330	0
	Influenza B virus (B/Washington/02/2019)	39	0
	Influenza A virus (A/Puerto Rico/8/1934(H1N1))	12	0
	Human adenovirus B1	12	0
STP-Saliva-514	Human adenovirus C2	111	0
	Respiratory syncytial virus (type A)	24	0
	Influenza B virus (B/Lee/1940)	13	0
	KI polyomavirus Stockholm 60	13	0
	Influenza B virus (B/Wisconsin/01/2010)	13	0

[a]Total number of bases observed for viral (partial) target using COVIDSeq Test kit (Illumina, San Diego, CA)

[b]Coverage per base within viral (partial) target using COVIDSeq Test kit (Illumina, San Diego, CA)

Table S3. Quantification results from initial detection of SARS-CoV-2 (at time of diatnosis) in vaccinated individuals

VAC-ID	Cq[ab]
STP-Saliva-11[b]	Not available
STP-Saliva-410[b]	Not available
STP-Saliva-409[b]	Not available
STP-Saliva-412[b]	Not available
STP-Saliva-413[b]	Not available
STP-Saliva-513[b]	Not available
STP-Saliva-411	Not available
STP-Saliva-512	Not available
STP-Saliva-511	36.48 CT
STP-Saliva-514	28.85 CT

423 [a]PCR quantification cycle
424 [c]Vaccinated individuals with 70% genome coverage at 50x sequencing coverage/site.
425 *

Table S2. GISAID author acknowledgment table.

We gratefully acknowledge the following Authors from the Originating laboratories responsible for obtaining the specimens, as well as the Submitting laboratories where the genome data were generated and shared via GISAID, on which this research is based.

All Submitters of data may be contacted directly via www.gisaid.org

Authors are sorted alphabetically.

Accession ID	Originating Laboratory	Submitting Laboratory	Authors
EPI_ISL_1225879, EPI_ISL_1226183, EPI_ISL_1226188	"AK State Public Health Lab, State Health Department"	Genomics and Discovery, Respiratory Viruses Branch, Division of Viral Diseases, Centers for Disease Control and Prevention	Anna Montmayeur; Anna Uehara; Ben L. Rambo-Martin; Clinton R. Paden; Dhwani Batra; Haibin Wang; Jasmine Padilla; Jing Zhang; Justin Lee; Katie Dillon; Krista Queen; Kristen Knipe; Kristine Lacek; Lori Rowe; Mark Burroughs; Matthew Schmerer; Mili Sheth; Peter W. Cook; Rachel Marine; Sam Shepard; Sarah Nobles; Shoshona Le; Suxiang Tong; Yan Li; Ying Tao
EPI_ISL_1226332, EPI_ISL_1226338	"OK Public Health Laboratory, Oklahoma State DOH"	Genomics and Discovery, Respiratory Viruses Branch, Division of Viral Diseases, Centers for Disease Control and Prevention	Anna Montmayeur; Anna Uehara; Ben L. Rambo-Martin; Clinton R. Paden; Dhwani Batra; Haibin Wang; Jasmine Padilla; Jing Zhang; Justin Lee; Katie Dillon; Krista Queen; Kristen Knipe; Kristine Lacek; Lori Rowe; Mark Burroughs; Matthew Schmerer; Mili Sheth; Peter W. Cook; Rachel Marine; Sam Shepard; Sarah Nobles; Shoshona Le; Suxiang Tong; Yan Li; Ying Tao
EPI_ISL_699655	1-Laboratory of Microbiology, National Reference Lab, Charles Nicolle Hospital; 2-University of Tunis ElManar, Faculty of Medicine of Tunis, LR99ES09, Tunis, Tunisia	1-Clinical and Experimental Pharmacology Lab, LR16SP02, National Center of Pharmacovigilance, University of Tunis El Manar, Tunis, Tunisia. 2-Neurodegenerative diseases and psychiatric troubles, LR18SP03, Razi Hospital, University of Tunis El Manar, Tunis, Tunisia. 3- Ministry of Health, National Observatory of New and Emerging Diseases, 1006, Tunis, Tunisia	Alia Ben Kahla; Asma Ferjani; Gaies Emna; Guedi Berrabeh; Hanen ElJebari; Ilhem Boutiba-Ben Boubaker; Jalila Ben Khelil; Maher Kharrat; Mouna Ben Sassi; Mouna Safer; Nissaf Ben Alaya; Riadh Daghfous; Riadh Gouider.; Salma Abid; Salwa Mrabet; Sameh Trabelsi; Sana Ferjani
EPI_ISL_1013566	1.AO Universitaria 'S. Giovanni di Dio e Ruggi D'Aragona, Scuola Medica Salernitana' Hospital / 2.UOC di Virologia e Microbiologia, Università della Campania 'L. Vanvitelli' / 3.AO Universitaria 'Federico II' Napoli Hospital / 4.AORN 'San Giuseppe Moscati' Avellino Hospital / 5.AO 'San Pio - presidio G. Rummo' Benevento Hospital / 6.AO 'Sant'Anna e San Sebastiano' Caserta Hospital / 7.PO 'Maria Santissima Addolorata' Eboli Hospital / 8.Biogem Istituto di Ricerche Genetiche	1. Genome Research Center for Health (CRGS) / 2. Laboratory of Molecular Medicine and Genomics(LMMGe) / 3. Center for Research in Pure and Applied Mathematics (CRMPA)	Alessandro Weisz; Alessia Cossu; Andreina Baj; Aniello Gentile; Annamaria Salvati; Antonello Saccomanno; Arnolfo Petruzziello; Assunta Sellitto; Carlo Ferravante; Domenico Memoli; Domenico Palumbo; Edmondo Adorisio; Elena Alexandrova; Emilia Vaccaro; Fausto Sessa.; Francesca Marciano; Francesca Rizzo; Francesco Curcio; Gianluigi Franci; Giorgio Dirani; Giorgio Giurato; Giovanni Nassa; Giovanni Pecoraro; Giuseppe Fenza; Giuseppe Portella; Gregorio Goffredi; Ilaria Terenzi; Jessica Lamberti; Maddalena Schioppa; Maria Grazia Foti; Maria Landi; Marianna Scrima; Mariarosaria Ingino; Massimiliano Galdiero; Maurizio Fumi; Michela Iacobellis; Michele Caraglia; Michele Cennamo; Morena D'Avenia; Oriana Strianese; Pasquale Pagliano; Rita Greco; Roberta Tarallo; Rosanna Piluscio; Silvia Zanoli; Simona Semprini; Sonia Amabile; Stefania Marzinotto; Teresa Rocco; Valeria Mirici Cappa; Vincenzo Rocco; Viola Melone; Vittoria Letizia; Vittorio Sambri; Ylenia D'Agostino
EPI_ISL_982502	ADIRONDACK MEDICAL CENTER	Wadsworth Center, New York State Department of Health	Alexis Russel; Daryl M. Lamson; Erasmus Schneider; Erica Lasek-Nesselquist; John Kelly; Jonathan Plitnick; Kirsten St. George; Matthew Shudt; Melissa A Leisner; Navjot Singh
EPI_ISL_1095229	AK State Public Health Lab, State Health Department	Respiratory Viruses Branch, Division of Viral Diseases, Centers for Disease Control and Prevention	Anna Montmayeur; Anna Uehara; Ben L. Rambo-Martin; Clinton R. Paden; Dhwani Batra; Haibin Wang; Jasmine Padilla; Jing Zhang; Justin Lee; Krista Queen; Lori Rowe; Mark Burroughs; Mili Sheth; Peter W. Cook; Rachel Marine; Sarah Nobles; Suxiang Tong; Yan Li; Ying Tao
EPI_ISL_1094818	AR Dept. of Health-Public Health Lab	Respiratory Viruses Branch, Division of Viral Diseases, Centers for Disease Control and Prevention	Anna Montmayeur; Anna Uehara; Ben L. Rambo-Martin; Clinton R. Paden; Dhwani Batra; Haibin Wang; Jasmine Padilla; Jing Zhang; Justin Lee; Krista Queen; Lori Rowe; Mark Burroughs; Mili Sheth; Peter W. Cook; Rachel Marine; Sarah Nobles; Suxiang Tong; Yan Li; Ying Tao
EPI_ISL_1166231, EPI_ISL_1166252	ASL Napoli 1 Centro	AMES Centro Polidiagnostico Strumentale S.r.l.	"Giovanni Savarese; Antonella Di Carlo; Antonio Fico"; Eloisa Evangelista; Luigi D'Amore; Luisa Circelli; Maurizio D'Amora; Monica Ianniello; Nadia Petrillo; Raffaella Ruggiero; Roberto Sirica
EPI_ISL_1027445, EPI_ISL_1027467, EPI_ISL_1235463, EPI_ISL_1235476	Alameda County Public Health Lab	Chan-Zuckerberg Biohub	CZB Cliahub Consortium
EPI_ISL_911688, EPI_ISL_1195922	Alaska State Virology Laboratory	Alaska State Virology Laboratory	Elva House; Jack Chen; Lisa Smith; Ph.D.; Stephanie DeRonde
EPI_ISL_933583, EPI_ISL_933589, EPI_ISL_967882, EPI_ISL_978486, EPI_ISL_1016924, EPI_ISL_1064177, EPI_ISL_1184559, EPI_ISL_1239095			
see above	Arizona State Public Health Laboratory	Arizona State Public Health Laboratory	Jessica Escobar; Katherine Fullerton; Linda Getsinger; Nobuko Fukushima; Stacy White; Trung Huynh; Victor Waddell
EPI_ISL_1118038	Austrian Agency for Health and Food Safety (AGES)	Bergthaler laboratory, CeMM Research Center for Molecular Medicine of the Austrian Academy of Sciences	Andreas Bergthaler; Anna Schedl; Bekir Erguner; Benedikt Agerer; Christoph Bock; Jan Laine; Lukas Endler; Maelle Le Moing; Martin Senekowitsch; Michael Schuster; Thomas Penz
EPI_ISL_884859	Bacteriology, Georgia Public Health Laboratory (GPHL)	Bacteriology, Georgia Public Health Laboratory (GPHL)	Dixey, C.; Edwards, J.; Parrott, T.; Reeves, S.
EPI_ISL_1081181	Baylor Scott & White-Temple	Baylor Scott & White-Temple	Ari Rao; Kimberly Walker; Linden Morales; Marcus Volz; Shelby Hendrickson
EPI_ISL_1049207	Blackhawk Genomics	Pathogen Discovery, Respiratory Viruses Branch, Division of Viral Diseases, Centers for Disease Control and Prevention	Anna Uehara; Brian Lynch; Clinton R. Paden; Haibin Wang; Han Jia Ng; Jing Zhang; Krista Queen; Peter Cook; Suxiang Tong; Yan Li; Ying Tao
EPI_ISL_1121640, EPI_ISL_1253808, EPI_ISL_1253817	Broad Institute Clinical Research Sequencing Platform	Infectious Disease Program, Broad Institute of Harvard and MIT	Adams, G.; B.L.; B.W.; Bauer, M.; Birren; Carter, A.; Chaluvadi, S.; D.J.; DeRuff, K.; Gallagher, G.; Gladden-Young, A.; J.E.; K.J.; Lagerborg, K.; Lemieux; Loreth, C.; MacInnis; Normandin, E.; P.C.; Park; Reilly, S.; Rudy, M.; Siddle; Smole, S.; Tomkins-Tinch, C.; and Sabeti
EPI_ISL_906885, EPI_ISL_906886, EPI_ISL_906887, EPI_ISL_906889, EPI_ISL_906891, EPI_ISL_906892, EPI_ISL_906894, EPI_ISL_906895, EPI_ISL_906897, EPI_ISL_906898, EPI_ISL_906899, EPI_ISL_906900, EPI_ISL_906903, EPI_ISL_906906, EPI_ISL_906908, EPI_ISL_906909, EPI_ISL_906913			
see above	Bureau of Public Health Laboratories, Florida Department of Health (BPHL, FLDOH)	Bureau of Public Health Laboratories, Florida Department of Health (BPHL, FLDOH)	Blanton, J.; Schmedes, S.
EPI_ISL_1225957	CA-Los Angeles County Public Health Laboratory	Genomics and Discovery, Respiratory Viruses Branch, Division of Viral Diseases, Centers for Disease Control and Prevention	Anna Montmayeur; Anna Uehara; Ben L. Rambo-Martin; Clinton R. Paden; Dhwani Batra; Haibin Wang; Jasmine Padilla; Jing Zhang; Justin Lee; Katie Dillon; Krista Queen; Kristen Knipe; Kristine Lacek; Lori Rowe; Mark Burroughs; Matthew Schmerer; Mili Sheth; Peter W. Cook; Rachel Marine; Sam Shepard; Sarah Nobles; Shoshona Le; Suxiang Tong; Yan Li; Ying Tao
EPI_ISL_1094478	CT-Dr. Katherine A. Kelley State Public Health Lab	Respiratory Viruses Branch, Division of Viral Diseases, Centers for Disease Control and Prevention	Anna Montmayeur; Anna Uehara; Ben L. Rambo-Martin; Clinton R. Paden; Dhwani Batra; Haibin Wang; Jasmine Padilla; Jing Zhang; Justin Lee; Krista Queen; Lori Rowe; Mark Burroughs; Mili Sheth; Peter W. Cook; Rachel Marine; Sarah Nobles; Suxiang Tong; Yan Li; Ying Tao
EPI_ISL_847665	California Department of Public Health	Chiu Laboratory, University of California, San Francisco	Brian Bushnell; Candace Wang; Charles Chiu; Debra Wadford; Jill Hacker; Scot Federman; Xianding (Wayne) Deng
EPI_ISL_824561, EPI_ISL_824679	Cedars-Sinai Medical Center, Department of Pathology & Laboratory Medicine, Molecular Pathology Laboratory	Cedars-Sinai Medical Center, Molecular Pathology Laboratory of Department of Pathology & Laboratory Medicine and Genomic Core	Brian Davis; Eric Vail; Jasmine T Plummer; Jorge Mario Sincuir Martinez; Stephanie Chen; Wenjuan Zhang
EPI_ISL_1168655, EPI_ISL_1168671	Centers for Disease Control and Prevention, Dengue Branch	Centers for Disease Control and Prevention, Dengue Branch	Betzabel Flores; Gabriela Paz-Bailey; Gilberto A. Santiago; Glenda Gonzalez; Jorge L. Munoz-Jordan; Keyla Charriez
EPI_ISL_961847	Centrala laboratorija	Latvian Biomedical Research and Study Centre	Davids Fridmanis; Ivars Silamikelis; Jana Osite; Janis Pjalkovskis; Janis Klovins; Jurijs Perevoscikovs; Kaspars Megnis; Laila Silamikele; Lauma Freimane; Laura Ansone; Liga Birzniece; Marta Priedite; Monta Ustinova; Nikita Zrelovs; Uga Dumpis; Vita Rovite
EPI_ISL_978135, EPI_ISL_978137	Chiu Laboratory, University of California, San Francisco	Chiu Laboratory, University of California, San Francisco	Candace Wang; Charles Chiu; Debra Wadford; Jill Hacker; Venice Servellita; Xianding (Wayne) Deng
EPI_ISL_1163754, EPI_ISL_1163791	Clinical Molecular Microbiology Laboratory, UNC Hospital	Dirk Dittmer	Angelica Juarez; Blossom Damania.; Brent A. Eason; Cameroon Grant; Carolina Caro-Vegas; Cecilia Thompson; Dirk Dittmer; Evelyn Hoffman; Jason Wong; Justin T. Landis; Linda Pluta; Melissa B. Miller; Patricio Cano; Razia Moorad; Ryan McNamara; Shawn Hawken
EPI_ISL_861455, EPI_ISL_911598,	Clinical Molecular Microbiology Laboratory, UNC Hospitals	Jeremy Wang	Alexander Rubinsteyn; Colleen Rice; Corbin Jones; Jason Smedberg; Jeremy Wang; Melissa Miller; Robert Hagan; Shawn Hawken

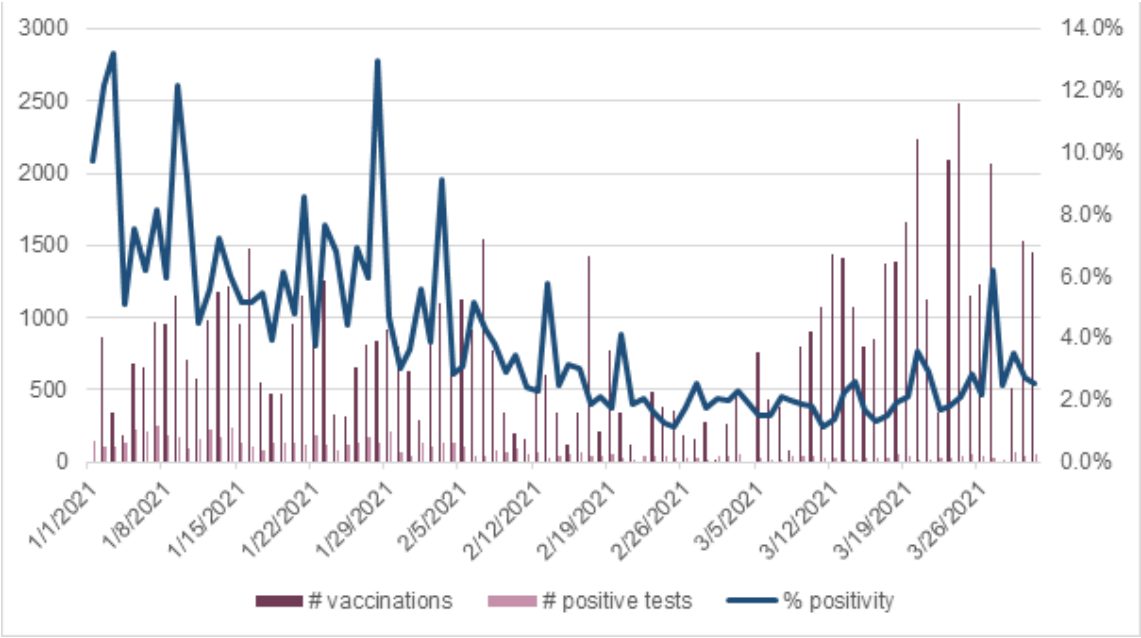

Figure S1. COVID-19 vaccinations and test positivity in Alachua County, Florida, from January 1st – March 31st, 2021.

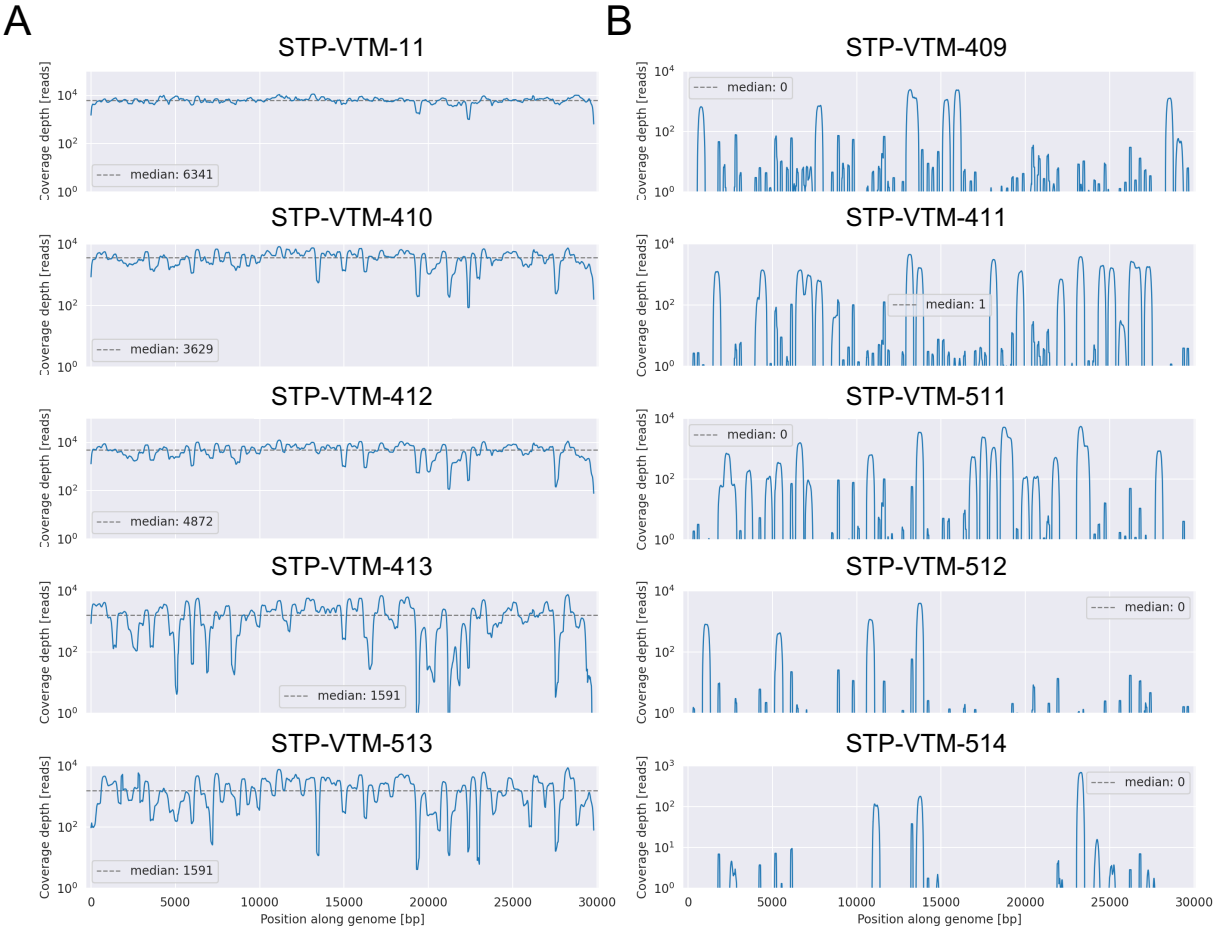

Figure S2. SARS-CoV-2 genome coverage for (A) five successfully and (B) five unsuccessfully sequenced vaccinated individuals. Coverage in this plot refers to the number of reads representing each position within the MN908947 reference SARS-CoV-2 genome and was provided by Illumina.

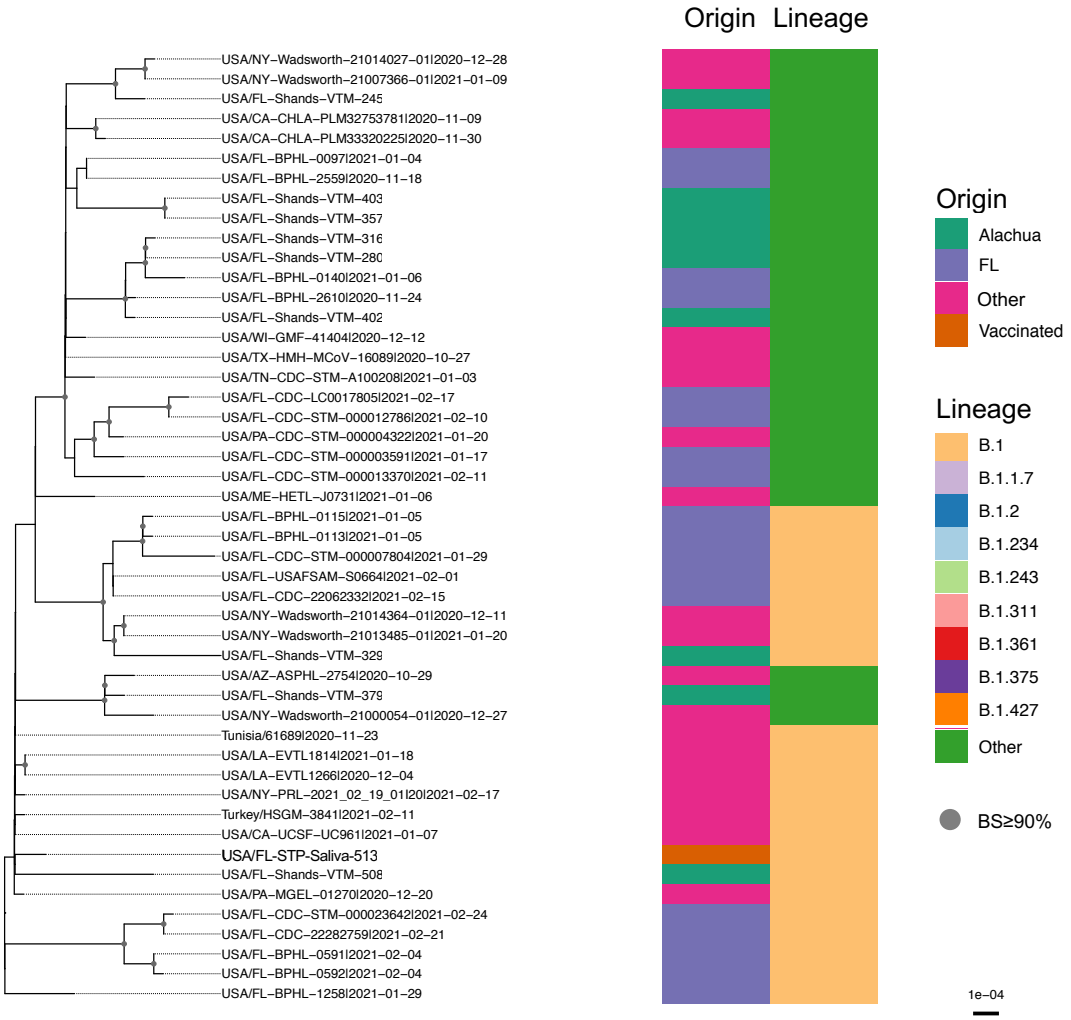

Figure S3. Distribution of identified lineages and geographical origin within a fragment of the phylogenetic tree containing FL-Shands-VTM-513 (B.1 lineage). Branches shown are scaled in genetic substitutions/site. Nodes with ≥90% support using bootstrap sampling are indicated by grey dots. This clade is not well-supported but represents a fragment of the tree in Figure 1 three nodes back from the FL-STP-Saliva-513 taxon. Other lineages represent lineages comprising <1% of the total sample population, though in this subtree only B.1.349 and B.1.363 are present.

References

1. Rambaut A, Loman N, Pybus O, Barclay W, Barrett J, Carabelli A, et al. Preliminary genomic characterisation of an emergent SARS-CoV-2 lineage in the UK defined by a novel set of spike mutations. Virologicalorg. 2020;https://virological.org/t/preliminary-genomic-characterisation-of-an-emergent-sars-cov-2-lineage-in-the-uk-defined-by-a-novel-set-of-spike-mutations/563.
2. Rambaut A, Holmes EC, O'Toole Á, Hill V, McCrone JT, Ruis C, et al. A dynamic nomenclature proposal for SARS-CoV-2 lineages to assist genomic epidemiology. Nat Microbiol. 2020;5(11):1403-7.

3. Larsen B, Worobey M. Phylogenetic evidence that B.1.1.7 has been circulating in the United States since early- to mid-November. Virologicalorg. 2021(https://virological.org/t/phylogenetic-evidence-that-b-1-1-7-has-been-circulating-in-the-united-states-since-early-to-mid-november/598).
4. Zhang W, Davis BD, Chen SS, Sincuir Martinez JM, Plummer JT, Vail E. Emergence of a Novel SARS-CoV-2 Variant in Southern California. JAMA. 2021;325(13):1324-6.
5. Hitchings MDT, Ranzani OT, Scaramuzzini Torres MS, de Oliveira SB, Almiron M, Said R, et al. Effectiveness of CoronaVac in the setting of high SARS-CoV-2 P.1 variant transmission in Brazil: A test-negative case-control study. medRxiv. 2021:2021.04.07.21255081.
6. Madhi SA, Baillie V, Cutland CL, Voysey M, Koen AL, Fairlie L, et al. Efficacy of the ChAdOx1 nCoV-19 Covid-19 Vaccine against the B.1.351 Variant. N Engl J Med. 2021.
7. Buss LF, Prete CA, Abrahim CMM, Mendrone A, Salomon T, de Almeida-Neto C, et al. Three-quarters attack rate of SARS-CoV-2 in the Brazilian Amazon during a largely unmitigated epidemic. Science. 2021;371(6526):288-92.
8. Sabino BD, Alonso FOM, Oliveira MSC, Venceslau MT, Guimarães MAAM, Varella RB. Long-term intermittent detection of SARS CoV 2 in the upper respiratory tract: what is the meaning of it? Infect Dis (Lond). 2021;53(2):151-3.
9. Polack FP, Thomas SJ, Kitchin N, Absalon J, Gurtman A, Lockhart S, et al. Safety and Efficacy of the BNT162b2 mRNA Covid-19 Vaccine. N Engl J Med. 2020;383(27):2603-15.
10. Alachua County COVID-19 Recovery Dashboard https://dashboards.alachuacounty.us/COVID19/
[
11. To KK, Tsang OT, Leung WS, Tam AR, Wu TC, Lung DC, et al. Temporal profiles of viral load in posterior oropharyngeal saliva samples and serum antibody responses during infection by SARS-CoV-2: an observational cohort study. Lancet Infect Dis. 2020;20(5):565-74.
12. Zhu J, Guo J, Xu Y, Chen X. Viral dynamics of SARS-CoV-2 in saliva from infected patients. J Infect. 2020;81(3):e48-e50.
13. Charre C, Ginevra C, Sabatier M, Regue H, Destras G, Brun S, et al. Evaluation of NGS-based approaches for SARS-CoV-2 whole genome characterisation. Virus Evol. 2020;6(2):veaa075.
14. Cevik M, Tate M, Lloyd O, Maraolo AE, Schafers J, Ho A. SARS-CoV-2, SARS-CoV, and MERS-CoV viral load dynamics, duration of viral shedding, and infectiousness: a systematic review and meta-analysis. Lancet Microbe. 2021;2(1):e13-e22.
15. Giovanetti M, Cella E, Benedetti F, Magalis BR, Fonseca V, Fabris S, et al. SARS-CoV-2 shifting transmission dynamics and hidden reservoirs limited the efficacy of public health interventions in Italy. medRxiv. 2020:2020.12.16.20248355.
16. Moreno G, Braun K, Larsen B, Alpert T, Worobey M, Grubaugh N, et al. Detection of non-B.1.1.7 Spike Δ69/70 sequences (B.1.375) in the United States. Virologicalorg. 2021 https://virological.org/t/detection-of-non-b-1-1-7-spike-69-70-sequences-b-1-375-in-the-united-states/587.
17. Minh BQ, Schmidt HA, Chernomor O, Schrempf D, Woodhams MD, von Haeseler A, et al. IQ-TREE 2: New Models and Efficient Methods for Phylogenetic Inference in the Genomic Era. Mol Biol Evol. 2020;37(5):1530-4.
18. Hoang DT, Chernomor O, von Haeseler A, Minh BQ, Vinh LS. UFBoot2: Improving the Ultrafast Bootstrap Approximation. Mol Biol Evol. 2018;35(2):518-22.
19. Minh BQ, Nguyen MA, von Haeseler A. Ultrafast approximation for phylogenetic bootstrap. Mol Biol Evol. 2013;30(5):1188-95.
20. Baden LR, El Sahly HM, Essink B, Kotloff K, Frey S, Novak R, et al. Efficacy and Safety of the mRNA-1273 SARS-CoV-2 Vaccine. N Engl J Med. 2021;384(5):403-16.
21. Sadoff J, Le Gars M, Shukarev G, Heerwegh D, Truyers C, de Groot AM, et al. Interim Results of a Phase 1-2a Trial of Ad26.COV2.S Covid-19 Vaccine. N Engl J Med. 2021.

501 22. Greaney AJ, Loes AN, Crawford KHD, Starr TN, Malone KD, Chu HY, et al. Comprehensive
502 mapping of mutations in the SARS-CoV-2 receptor-binding domain that affect recognition by polyclonal
503 human plasma antibodies. Cell Host Microbe. 2021;29(3):463-76.e6.
504 23. Suryadevara N, Shrihari S, Gilchuk P, VanBlargan LA, Binshtein E, Zost SJ, et al. Neutralizing and
505 protective human monoclonal antibodies recognizing the N-terminal domain of the SARS-CoV-2 spike
506 protein. Cell. 2021.
507 24. Ostrov D. Structural consequences of variation in SARS-CoV-2 B.1.1. Scientific Archives.
508 2021;3(2):103-8.
509 25. Wu K, Werner AP, Koch M, Choi A, Narayanan E, Stewart-Jones GBE, et al. Serum Neutralizing
510 Activity Elicited by mRNA-1273 Vaccine. N Engl J Med. 2021.
511 26. Wang P, Nair MS, Liu L, Iketani S, Luo Y, Guo Y, et al. Antibody resistance of SARS-CoV-2 variants
512 B.1.351 and B.1.1.7. Nature. 2021.
513 27. Kustin T, Harel N, Finkel U, Perchik S, Harari S, Tahor M, et al. Evidence for increased
514 breakthrough rates of SARS-CoV-2 variants of concern in BNT162b2 mRNA vaccinated individuals.
515 medRxiv. 2021:2021.04.06.21254882.
516 28. Altschul SF, Gish W, Miller W, Myers EW, Lipman DJ. Basic local alignment search tool. J Mol
517 Biol. 1990;215(3):403-10.
518 29. Moshiri N. ViralMSA: Massively scalable reference-guided multiple sequence alignment of viral
519 genomes. Bioinformatics. 2020.
520 30. Lednicky JA, Lauzardo M, Fan ZH, Jutla A, Tilly TB, Gangwar M, et al. Viable SARS-CoV-2 in the air
521 of a hospital room with COVID-19 patients. Int J Infect Dis. 2020;100:476-82.
522 31. Lednicky JA, Cherabuddi K, Tagliamonte MS, Elbadry MA, Subramaniam K, Waltzek TB, et al. In-
523 Frame 12-Nucleotide Deletion within Open Reading Frame 3a in a SARS-CoV-2 Strain Isolated from a
524 Patient Hospitalized with COVID-19. Microbiol Resour Announc. 2021;10(8).
525 32. Carbone M, Lednicky J, Xiao SY, Venditti M, Bucci E. Coronavirus 2019 Infectious Disease
526 Epidemic: Where We Are, What Can Be Done and Hope For. J Thorac Oncol. 2021;16(4):546-71.
527 33. Lednicky JA, Lauzardo M, Alam MM, Elbadry MA, Stephenson CJ, Gibson JC, et al. Isolation of
528 SARS-CoV-2 from the air in a car driven by a COVID patient with mild illness. Int J Infect Dis. 2021.
529 34. CDC. CDC real-time reverse transcriptase PCR (rRT-PCR) diagnostic test for COVID-19
530 https://www.cdc.gov/coronavirus/2019-ncov/lab/virus-requests.html [

531